A Center of Mass Estimation and Control Strategy for Body-Weight-Support Treadmill Training

Xinwei Li, Bingze He, Zhipeng Deng, Yixi Chen, Duojin Wang, Yuanjie Fan, Hao Su, and Hongliu Yu

***Abstract*— Walking disorders are common in post-stroke. Body weight support (BWS) systems have been proposed and proven to enhance gait training systems for recovering in individuals with hemiplegia. However, the fixed weight support and walking speed increase the risk of falling and decrease the active participation of the subjects. This paper proposes a strategy to enhance the efficiency of BWS treadmill training. It consists in regulating the height of the BWS system to track the height of the subject's center of mass (CoM), whereby the CoM is estimated through a long-short term memory (LSTM) network and a locomotion recognition system. The LSTM network takes the walking speed, body-height to leg-length ratio, hip and knee joint angles of the hemiplegic subjects' non-paretic side from the locomotion recognition system as input signals and outputs the CoM height to a BWS treadmill training robot. Besides, the hip and knee joints' ranges of motion are increased by 34.54% and 25.64% under the CoM height regulation compared to the constant weight support, respectively. With the CoM height regulation strategy, the stance phase duration of the paretic side is significantly increased by 14.6% of the gait cycle, and the symmetry of the gait is also promoted. The CoM height kinematics by adjustment strategy is in good agreement with the mean values of the 14 non-disabled subjects, which demonstrated that the adjustment strategy improves the stability of CoM height during the training.**

***Index Terms*— Body weight support, center of mass height, locomotion recognition, long-short term memory, post-stroke.**

I. Introduction

AROUND 15% of the global population is disabled, according to the World Health Organization (WHO), and more than six million people die each year because of stroke [1]. Amongst other pathologies, walking dysfunction is a major problem for many subjects who have suffered a stroke [2]–[4]. Walking disorders can lead to falls and restrict the stroke patient from performing daily living activities. Therefore, a primary objective of stroke rehabilitation in clinical practice is to improve independent walking [5]. To date, a clinical study that includes several meta-analyses of controlled randomized trials indicates that a variety of motor rehabilitation strategies such as electromechanical gait trainers, partial body weight supported treadmill training, and speed-dependent treadmill training are beneficial for achieving gains in walking speed and distance when compared to overground walking training [6]. There is emerging evidence that intensive, repetitive, and task-oriented training can reduce neurological deficits, which leads to short- and long-term cortical reorganization [7], [8]. Effective treadmill walking training can speed up the process of nerve remodeling for post-stroke patients [9], [10]. However, patients' motion control on lower limb joints is not effective due to the unstable muscle strength of one side of hemiplegia, which results in the difficulty of achieving repetitive walking training.

For the past few years, body weight support (BWS) systems have been proposed and proven to enhance gait training systems for patients recovering from spinal cord injury or stroke [7], [11]–[13]. Treadmill training is a promising treatment strategy because it allows the repetitive practice of complex gait cycles [14]. It is postulated to benefit locomotion by enhancing repetitive stepping practice and task-specific training, when compared to traditional overground training sessions supervised by physiotherapists [15]. Manual treadmill training conducted by physiotherapists has been demonstrated as an effective rehabilitation treatment for improving the gait speed and walking distance for stroke patients. The conventional BWS treadmill training requires a team of three or more physical therapists to guide the patient's legs on predefined paths and to stabilize the patient's pelvis [16]. The quality of manually assisted BWS treadmill training is dependent on the therapist's experience and judgment, which varies widely amongst therapists [17]. Also, the training sessions are short due to the physical therapist's fatigue and do not have any proper method of recording the patient's progress, and recovery [18].

Automated rehabilitation solutions are investigated lately to overcome the above-mentioned shortcomings of manual

Manuscript received April 5, 2021; revised August 13, 2021 and October 25, 2021; accepted November 3, 2021. Date of publication November 8, 2021; date of current version November 17, 2021. This work was supported in part by the National Natural Science Foundation of China under Grant 62073224. *(Corresponding author: Hongliu Yu.)*

This work involved human subjects or animals in its research. Approval of all ethical and experimental procedures and protocols was granted by the Review Board of Huashan Hospital under Application No. 2019017.

Xinwei Li, Bingze He, Zhipeng Deng, Yixi Chen, and Duojin Wang are with the School of Health Science and Engineering, University of Shanghai for Science and Technology, Shanghai 200093, China.

Yuanjie Fan is with the Shanghai Electric Central Research Institute, Shanghai 200070, China.

Hao Su is with the Laboratory of Biomechatronics and Intelligent Robotics, Department of Mechanical and Aerospace Engineering, North Carolina State University, Raleigh, NC 27695 USA.

Hongliu Yu is with the Shanghai Engineering Research Center of Assistive Devices, School of Health Science and Engineering, University of Shanghai for Science and Technology, Shanghai 200093, China (e-mail: yhl98@hotmail.com).

Digital Object Identifier 10.1109/TNSRE.2021.3126104

This work is licensed under a Creative Commons Attribution 4.0 License. For more information, see https://creativecommons.org/licenses/by/4.0/

physical therapy [19]. More specifically, robot-assisted gait training is used to counteract gait disorders in recent years [3], [20]. In clinical practice, robots such as the Lokomat (Hocoma, Volketswil, Switzerland) [21], Gait Trainer GT II (Reha Stim, Berlin, Germany) [22], Lyra (Thera Trainer, Hochdorf, Germany) [23], [24] and KineAssist (Woodway, Waukesha, America) [24] are used for BWS treadmill training. The benefit of these treadmill training systems is twofold: (1) the robot's BWS system carries the patient's weight, and (2) the gait pattern is induced by a specific robot strategy that releases the therapists from physical labor. Patients receiving electromechanically assisted gait training in combination with post-stroke physiotherapy are more likely to recover independent walking than patients receiving gait training without these devices [22]. Despite the benefits of robot-assisted gait preparation, this therapeutic approach often presented some disadvantages. The system of BWS partly reduced muscle function and restricted the degrees of freedom of the leg and pelvis movement, leading to abnormal changes in the patterns of muscle activation [25]. Optimization of robot-assisted rehabilitation devices is essential in overcoming the disadvantages mentioned above.

Novel robotic techniques, such as the biofeedback mode of the Lyra [23], the released mode of the Lokomat [22], the modification of the guiding force, and the active-assistive mode of the G-EO [22], strive to promote healing by enabling the subject to effectively control the robot-assisted gait training using their residual muscle movement. Another effective approach for the BWS treadmill training is varying the BWS harness height with a predefined trajectory that is determined by the ratio between the lower limb length and the height of the stroke subjects [6]. Post-stroke subjects with hemiplegia can be trained by their own active movement considering the contralateral side's motion information because the lower extremity of their non-paretic side maintains walking capability.

Human gait consists of a repeated sequence of basic limb motions to move the body along the desired direction while maintaining weight-bearing stability, conserving energy, and absorbing the floor shocks. From a mechanical point of view, the body can be represented by its center of mass (CoM), whose trajectory describes how the whole body progresses/moves [2], [26]. The track of the CoM moving up and down can improve patients' active participation in BWS treadmill training, which is a control method in line with the physiology of human movement [27]. In addition to the force interaction and electrical stimulation, the BWS harness height adjustment strategy can be obtained from analyzing movement information of the healthy side in real-time. To realize the BWS training strategy based on the height of the CoM, how to obtain the trajectory of the human CoM is a priority issue to be solved. In [28], a quaternion was used in combination with an integrated approach to transform translatory accelerations of the CoM from an inertial measurement unit (IMU) during walking from the object system onto the global frame. A method was proposed for analyzing gait patterns determined by CoM through inertial sensors embedded in smart devices [29]. It employed an extended Kalman filter in conjunction with a quaternion approach to transforming accelerations from the object onto the global frame.

In this paper, a strategy for variable CoM height adjustment is proposed to enhance the efficiency of BWS treadmill training of hemiplegic patients after stroke. Taking the kinematic information of the hemiplegic patients' non-paretic side as the main input parameters for the CoM height adjustment would improve the patients' training participation. The hip and knee angles are calculated by a locomotion recognition system with five IMUs. The non-paretic side's kinematic information of the subjects is used for the CoM height estimation, and the paretic side's information is utilized for rehabilitation evaluation. The CoM height estimation algorithm is applied to a BWS treadmill training robot (NaturaGait, Shanghai Electric, China) as shown in Fig. 1. NaturaGait is mainly used for rehabilitation of individuals with lower limb dysfunction caused by motor nerve injury, cerebral injury, especially stroke. The CoM height of the BWS treadmill training robot is calculated by parameters from the subject's lower limbs. With the adaptive CoM height estimation strategy, the stroke patients can participate in the BWS treadmill training actively adapting to the walking speed.

The existing method using CoM focused mostly on the ratio of body weight for vertical impedance, adjusting the CoM height in BWSTT based on CoM height estimation for post-stroke rehabilitation has not been investigated. The contribution of this work is twofold: first, we proposed a method for CoM height estimation by lower limb kinematics. Second, we validated the effectiveness of adaptively adjusting the CoM height based on the active movement of the non-paretic side for the BWS treadmill training in post-stroke rehabilitation. The long short term memory (LSTM) neural network integrated with CoM estimation using periodicity information solves the gradient disappearance or explosion of the recurrent neural network (RNN), improves the network's ability to process long sequence data, and serves as a powerful tool for parameter prediction in the BWS treadmill training. The proposed strategy in BWS treadmill training for post-stroke patients using non-paretic lower limb kinematic information is able to provide a more precise and robust CoM height estimation for use in rehabilitation.

II. Materials and Methods

For patients with hemiplegia, the motor function of the healthy side is preserved. Therefore, to assist post-stroke patients in BWS treadmill training, the healthy side movement is treated as the reference expression of the active movement and is used to identify the patient's intention to move. Then, the mapping relationship between the kinematic information of lower limbs and the change of CoM height is established and used to dynamically adjust the upper and lower positions of the pelvic elevator during treadmill walking training.

A. Locomotion Recognition System

1) IMUs Mounting Position and Orientation: The locomotion recognition system integrates five IMUs (LPMS-ME1, Alubi, China), two of them are attached to the healthy side while

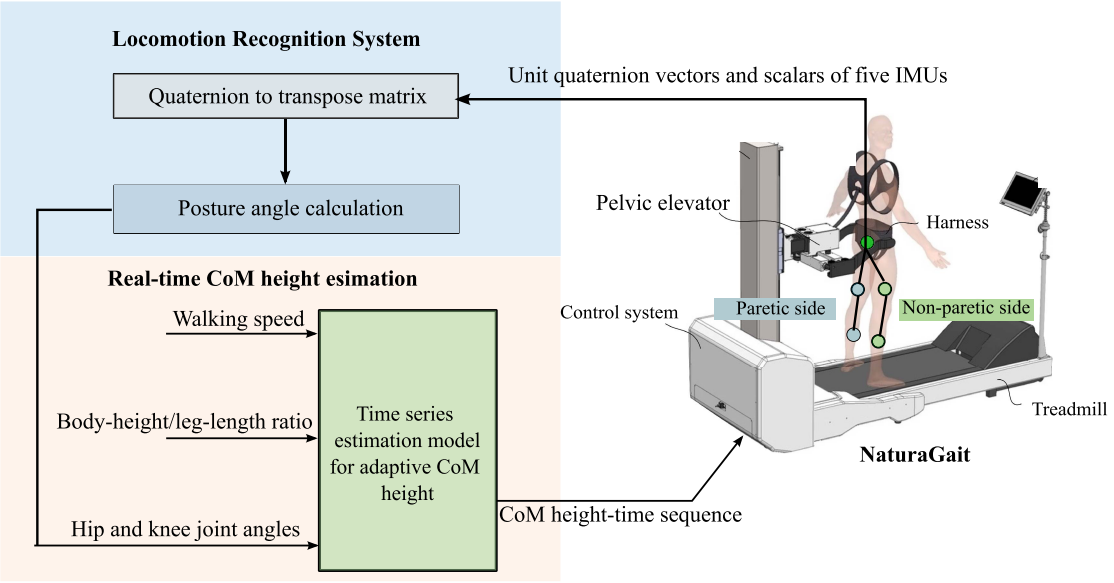

Fig. 1. System Overview of the adaptive CoM height adjustment strategy. The strategy consists of a locomotion recognition system, a center of mass (CoM) height estimation algorithm, and a BWS treadmill training robot. The CoM height estimation algorithm takes the walking speed, body-height, leg-length ratio, hip and knee joint angles of the hemiplegic subjects' non-paretic side from the locomotion recognition system as input signals and outputs the CoM height to a BWS treadmill training robot for rehabilitation training.

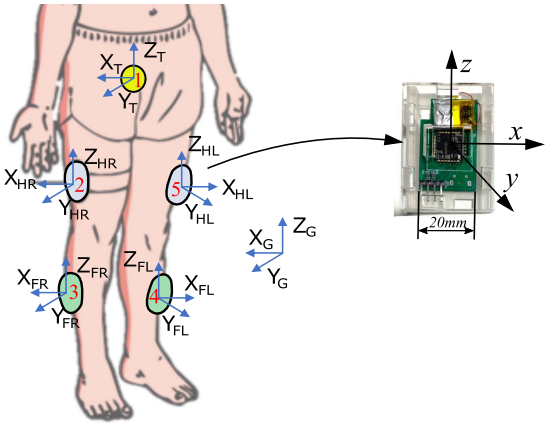

Fig. 2. Visualization of the IMUs coordinate systems and the global coordinate system. The locomotion recognition system consists of five IMUs, of which one is attached to the waist. Two IMUs are attached to the healthy side for CoM height estimation, and the other two are attached to the paretic side for motion assessment. IMUs on the left side and right side are arranged symmetrically.

one is attached to the waist for CoM height estimation, and the other two are attached to the paretic side for motion capture and rehabilitation assessment, as shown in Fig. 2. The quaternions are collected from the IMUs at a sampling rate of 100 Hz. The global coordinate system (X_G, Y_G, Z_G) is defined so that the x-axis lies in the horizontal plane and points to the right of the subject, while the z-axis points upwards. The waist IMU is located on the back of the pelvic. The z-axis of the IMU, Z_T, is aligned along the direction of the upward lumbar, and the x-axis, X_T, is perpendicular to the sagittal plane of the subject. On the right side of the lower limbs, the thigh IMU is placed on the outer and middle height of the thigh. The z-axis of the thigh IMU, Z_{HR}, is aligned along the direction of the upward femur, and the x-axis, X_{HR}, is perpendicular to the sagittal plane of the subject. The shank IMU is placed on the outer and middle height of the shank. The z-axis of the shank IMU, Z_{FR}, is aligned along the direction of the upward tibia, and the x-axis, X_{FR}, is perpendicular to the sagittal plane of the subject. Similarly, the two IMUs on the left side are arranged symmetrically. Since the IMU hardware is universally designed, the z-axis directions of the left and right thigh IMU are opposite, as shown in Fig. 2. The initialization posture of each IMU can be reset in a sensor setup software, the z-axis direction is set according to the wearing side is left or right.

2) Lower Limb Joint Angle Calculation: In the system initialization, the subjects were directed to keep their standing posture for three seconds after wearing the detection device for posture calibration and calculate the deviation attitude joint angle through the calibration attitude data. The initial calibration posture should be decoupled to obtain joint angle in the subsequent motion calculation. In the rest of our work, the whole calibration process does not require the use of third-party motion capture equipment. We tested this method with the third-party motion capture device by walking motion analysis at the same time, the experimental results showed that in addition to the individual attitude algorithm of angle motion capture system are biased with a third party. Our attitude detection system can meet the requirements in data periodicity and joint angles for the CoM height estimation. The initial relative posture between the IMU on the thigh and femur, $\mathbf{R}^i_{UH}$, and the relative posture matrix between the IMU on the shank and tibia, $\mathbf{R}^i_{LF}$, in the global coordinate system can be described as

$$\mathbf{R}^i_{UH} = \left(\mathbf{R}^i_{GU}\right)^{\mathrm{T}} \mathbf{R}^i_{GH}, \quad \mathbf{R}^i_{LF} = \left(\mathbf{R}^i_{GL}\right)^{\mathrm{T}} \mathbf{R}^i_{GF} \tag{1}$$

where the subscript U and L represent the coordinate of the IMU on the thigh and shank, respectively. The subscript H and F represent the coordinate of the femur and

tibia, respectively, while the superscript i refers to the initial configuration.

When the hip joint moves to a new position, n, the posture of the femur and tibia in the global coordinate can be described as

$$\mathbf{R}^n_{GH} = \mathbf{R}^n_{GU}\mathbf{R}^i_{UH}, \quad \mathbf{R}^n_{GF} = \mathbf{R}^n_{GL}\mathbf{R}^i_{LF} \tag{2}$$

A unit quaternion $\mathbf{q} = [x, y, z, w]^T$ can be obtained from the IMU with a vector, (x, y, z), and a scalar, w,

$$\mathbf{q} = x\mathbf{i} + y\mathbf{j} + z\mathbf{k} + w \tag{3}$$

The transpose of the femur rotation matrix in global coordinates is expressed as

$$(\mathbf{R}^n_{GH})^T = \begin{bmatrix} 1-2\left(y^2+z^2\right) & 2(xy-wz) & 2(wy+xz) \\ 2(xy+wz) & 1-2\left(x^2+z^2\right) & 2(yz-wx) \\ 2(xz-wy) & 2(wx+yz) & 1-2\left(x^2+y^2\right) \end{bmatrix} \tag{4}$$

and the relative Euler angles, γ, β and α, between the coordinates of femur and tibia pitch, roll, and yaw (joint flexion/extension in the sagittal plane, adduction/abduction in the frontal plane, and internal/external rotation).

$$\begin{aligned} \mathbf{R}^n_{GH} &= \mathbf{R}_Z(\alpha)\mathbf{R}_Y(\beta)\mathbf{R}_X(\gamma) \\ &= \begin{bmatrix} c\alpha c\beta & c\alpha s\beta s\gamma - s\alpha c\gamma & \cos\beta c\gamma + s\alpha s\gamma \\ s\alpha c\beta & s\alpha s\beta s\gamma + c\alpha c\gamma & s\alpha s\beta c\gamma - c\alpha s\gamma \\ -s\beta & c\beta s\gamma & c\beta c\gamma \end{bmatrix} \end{aligned} \tag{5}$$

where $c\alpha$ and $s\alpha$ are the abbreviation of $cos\alpha$ and $sin\alpha$, respectively.

The joint flexion/extension in the sagittal plane, α, adduction/abduction in frontal plane, β, and internal/external rotation, γ, are denoted by

$$\alpha = Atan2\left(r_{23}/s\beta, r_{13}/s\beta\right) \tag{6}$$

$$\beta = Atan2\left(\sqrt{r^2_{31} + r^2_{32}}, r_{33}\right) \tag{7}$$

$$\gamma = Atan2\left(r_{32}/s\beta, -r_{31}/s\beta\right) \tag{8}$$

where r_{ij} are the elements of $\mathbf{R}^n_{GH}$. The motion of hip and knee joints in the sagittal plane are the main parameters for the CoM height estimation, which is described in the next subsection.

In this work, the accuracy problem is analyzed as common works on motion capture which utilizes IMUs as wearable sensors [30]. Firstly, the IMUs are placed at a designated location on the waist, shank, and thigh of each subject. The location error of sensors is treated as a systematic error as it cannot be eliminated by initial calibration. Secondly, the performance parameters, zero-point drift and temperature drift, cannot be overlooked. The locomotion recognition system calibration parameters need to be reset when it has been used for more than 30 mins to avoid error accumulation.

B. LSTM for CoM Height Estimation

The nonlinear relationship between the healthy side data and the center of gravity's height in the whole gait cycle is observed. Therefore, in the application process, the data collected from the paretic side is mainly used as an evaluation index. During human walking, the lower limb joint parameters present obvious periodicity. Time domain's correlation with lower limb joint parameters is continuously changing. The CoM height estimation algorithm needs the memory capacity to process the time domain parameters and utilize the historical information. An RNN, one category of artificial neural networks wherein connections among nodes form a directed graph along with a temporal series, is adapted in the algorithm to showcase the temporal dynamic behavior of the parameters [31].

Derived from feedforward neural networks, RNNs can use their internal state (memory) to process variable-length sequences of inputs. Whereas, there are two main problems for RNN to estimate CoM height sequence with lower limb joint parameters in continuous treadmill training, (1) gradient vanishing and exploding problems, (2) it cannot process very long sequences if using hyperbolic tangent ($tanh$) or rectified linear unit ($relu$) as neural network activation function. This work relies on a variation of RNN called LSTM to address these challenges. The LSTM network adds thresholds input gate, forget gate, output gate, and memory units, solves the problem of gradient disappearance or explosion of the RNN, improving the network's ability to process long sequence data [32]. The difference between LSTM and an ordinary neural network is that the nodes between the hidden layers are connected, i.e., the input of the hidden layer at the given time not only contains the output of the hidden layer prior to the given time but also includes the output of the same hidden layer at the previous time. The historical information of the time series is stored in the network hidden layer. The LSTM can be used as a powerful tool to process sequence data. Therefore, the LSTM network is utilized to process the lower limb joint angles as they are time-series signals and is selected as the regression parameter prediction model. Since the lower limb joint angles we collect are a time-series signal, the LSTM network can be utilized to process the lower limb joint angles.

The LSTM advances traditional classifiers such as support vector machines by capturing feature vectors conveniently and automatically. Therefore, LSTM is selected as the regression parameter prediction model. The input parameters include angles of the hip and knee joint, real-time walking speed from NaturaGait, and leg length ratio to height. The model output of the LSTM is the predicted pelvis height, which is then sent to NaturaGait for height lifting device position and speed control.

The LSTM model for CoM height estimation is shown in Fig. 3, where x is the input eigenvector of the current cell, h_{t-1} is the output of the last cell, σ is the sigmoid function, z_f is the forget gate for information to be abandoned, c_t is the unit before the update, and the output value of f is a real number between 0 and 1; 0 means to forget all the information of the previous cell unit and one means to retain all the information of the previous cell unit and input the output value to c_{t-1}. The information is discarded when the input information passes through the forget gate. The input gate consists of a sigmoid layer and a $tanh$ layer. The sigmoid layer is responsible for information that requires an update, and the $tanh$ layer is responsible for creating the vector of

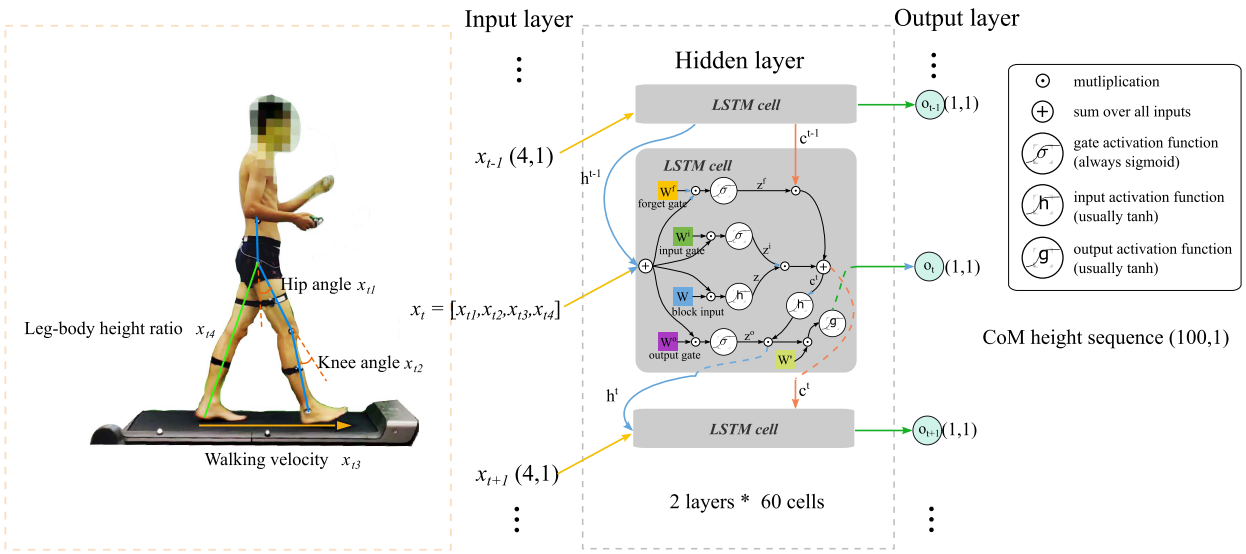

Fig. 3. Schematic diagram of neural network-based LSTM structure. The input layer (4,1) of the LSTM neural network includes leg-body height ratio, walking velocity, hip and knee angles. The output of the LSTM neural network is the CoM height sequence (100,1) for robot trajectory planning.

the alternative update content. The calculation of input gate and forget gate are defined as

$$z_i = \sigma\left(W^i(x_t + h_{t-1}) + b_i\right) \tag{9}$$

$$z_f = \sigma\left(W^f(x_t + h_{t-1}) + b_f\right) \tag{10}$$

After the information passes through the forget gate and input gate, the old cell state c_{t-1} will be updated to c_t as

$$c_t = z_f c_{t-1} + i_t\left(\tanh\left(W(x_t + h_{t-1}) + b\right)\right) \tag{11}$$

Then the output gate is integrated with a sigmoid layer and a *tanh* layer. The sigmoid layer determines which input information needs to be output. The *tanh* layer processes the information of the cell state. The output gate combines the sigmoid and *tanh* layer as the output,

$$o_t = \sigma\left(W^o(x_t + h_{t-1}) + b_o\right) \tag{12}$$

where W^f, W^i, W^o, W represent the weights of the input of the current eigenvector through each control gate and b_f, b_i, b_o, b represent the bias terms of the control gate.

The developed LSTM network parameters, such as the number of neurons, transfer function, and learning rate, are determined based on trial and CoM height estimation error to minimize the mean-square-error values to avoid over-or under-fitting as shown in TABLE.I. The model implementation is performed using MATLAB R2020b version (The Mathworks, Inc., Natick, MA, USA) and GTX 1660 Ti GPU (1536 CUDA cores, 1500 MHz base clock speed, and 12 GB RAM). Finally, the performance of the trained model is evaluated by ten-fold cross-validation.

The acceleration of lower limb joints is unstable during walking, which leads to the mutation of joint angle, especially for the hemiplegic subjects. The objective of stable walking training is that the change of center of gravity of subjects can have better periodicity in stable walking speed. In our method, we assume the consecutive two gait cycles share the same velocity, and the CoM height curve of the next gait cycle is estimated using the kinematics of the previous gait cycle immediately (within 10 ms) after the previous gait cycle is completed. Therefore, if a patient varies his or her walking in a specific cycle, the CoM height curve will be adjusted and recalculated in the next gait cycle. In our low-speed walking experiment, this delay did not have a significant influence on the performance of our method.

The velocity break needs to be averted in the treadmill waking training which means the waking velocity is stable in training. Since the hip joint angle has only one peak in each gait cycle, the continuous gait cycles are separated by the hip joint angle and angular velocity. The kinematic information of the previous cycle is treated as the input of the trained LSTM model to estimate the CoM height data of the next gait cycle. The CoM height estimation process takes 10ms, which does not affect the real-time performance of the system. The center of mass height estimation system sends NaturaGait a full gait cycle height change data and path planning at a fixed frequency, consisting of 100 position coordinates and 99-time parameters.

TABLE I
PARAMETERS DESIGN VALUES FOR LSTM

Parameters	Values
Training set size	6600
ratio of training/validation/test	70%:15%:15%
Input data dimension	(4,1)
Number of hidden layer	2
Number of hidden units	120
Training times	100
Batch size	30
Number of iterations/per training	15
Gradient descent	SGDM
Learning rate	0.01
L2 regularization coefficient	0.0001
Loss function	Cross-entropy
Weight initialization mode	Gaussian distribution

TABLE II
CHARACTERISTICS OF THE RECRUITED POST-STROKE SUBJECTS

Muscle strength level	Participant	Sex (M/F)	Age (years)	Height (cm)	L/H ratio	Weight (kg)	Side of paresis	Months Post-stroke
Level IV	S11	F	55	157	0.552	45.9	Right	20
	S12	F	63	162	0.543	50.2	Left	34
	S13	M	59	172	0.552	61.8	Left	20
	S14	M	46	188	0.521	75.2	Right	17
	Mean	\	55.75	169.75	0.542	58.3	\	22.75
Level III	S21	F	53	175	0.568	65.1	Right	13
	S22	M	63	176	0.575	61.3	Left	10
	S23	M	62	181	0.556	53.7	Left	6
	Mean	\	59.33	177.33	0.566	60.0	\	9.67
	Total Mean	\	57.29	173.00	0.552429	59.0	\	17.14

- M, male; F, female; L/H, leg-length/body-height

III. EXPERIMENTS

A. Experimental Protocol

In the CoM height estimation model training and validation experiments, we recruited eleven healthy subjects (two females and nine males, age: 26.2 ± 1.5 years, height: $171.2 \pm 4.3\ cm$, weight: $67.3 \pm 7.1\ kg$) for the model training experiments. Data from the eleven subjects were used for training and validation of the CoM height estimation model in Matlab, other three healthy subjects were recruited (one female, two males, age: 25.7 ± 1.2 years, height: $169.2 \pm 3.8\ cm$, weight: $65.9 \pm 3.3\ kg$) for the model testing experiments. The experiments were approved by the local ethics committee and performed at the Rehabilitation Engineering Laboratory in the University of Shanghai for Science and Technology. All participants provided written informed consent prior to the experiments. The walking speeds were set from $0.4m/s$ to $1.8m/s$ with an interval of $0.2m/s$. The wide range of walking speed covers all the common BWS training speeds and enhances the accuracy of the LSTM network. The 3D trajectories of 14 reflective markers located on the lower limbs were recorded using 12 infrared cameras motion analysis system (Vicon MX13, Oxford Metrics, UK) at a sampling rate of 100 Hz. The Plug-in Gait model was used for marker labeling, gaps in the trajectories were filled with appropriate gap-filling algorithms provided by Vicon Nexus.

In the CoM height estimation model testing and effectiveness validation for BWS training, we recruited seven hemiplegic subjects to walk with the BWS robot under the CoM height estimation and constant partial BWS strategies. According to the Lovett muscle strength scale, the selected subjects were divided into two groups by their lower limb muscle strength, Level IV and Level III. The characteristics of the seven subjects can be seen in Table II. The validation experiment scenes can be seen in Fig. 4. The subjects were trained with the VCHA and constant BWS modes under different walking speeds with the assistance of an experienced physical therapist for two days ($1.5h \sim 2h/day$) to evaluate the differences between the BWS with constant and variable CoM height strategies. The walking training speeds were set as $0.8m/s$, $1.0m/s$, $1.2m/s$.

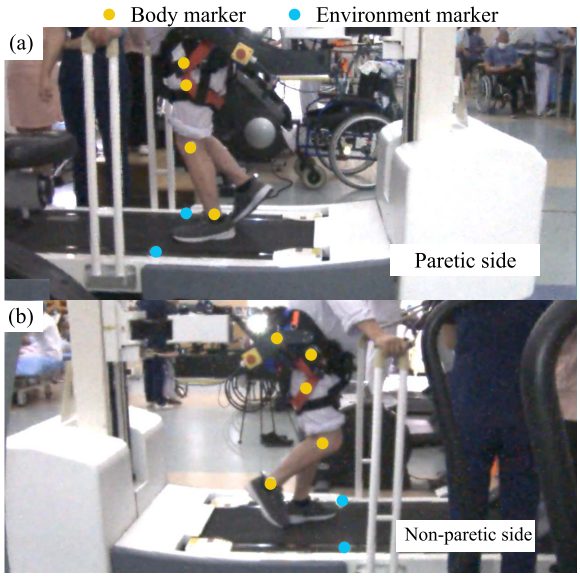

Fig. 4. A hemiplegic subject using the NaturaGait-based body weight support treadmill training system. The nine yellow points indicate the placements of the reflective markers on both the paretic (a) and healthy (b) sides of the subject. The remaining five markers are not in either view of the above two sub-figures.

The hemiplegic subjects were fixed on the robot by a wearable harness and received constant BWS treadmill training. The support ratios were 0.2 (Level IV) and 0.4 (Level III), which means that the robot applied a constant vertical force (20% and 40% of body weight) to the patient. The hemiplegic subjects were asked to hold on side supports as soft as possible to eliminate the influence from supports while ensuring their safety.

The 20% and 40% partial BWS were set as the reference strategy for the validation of the CoM height adjustment strategy in further analysis. The foot pressure and gait phase were measured by a wireless insole system (X4, Xsensor, Calgary, Canada) at a sampling rate of 100 Hz. The kinematic reference performance was recorded by Vicon MX13 at the same sampling rate of the insole system. The nine yellow points indicate the placements of the reflective markers on both

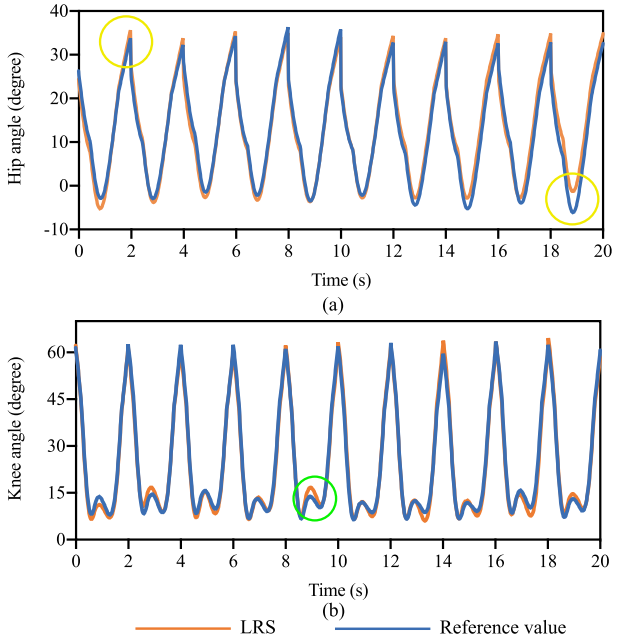

Fig. 5. Hip and knee joint angles of five gait cycles estimation from the locomotion recognition system compared to reference values from motion capture system at 1m/s. (a) The errors in peak and valley of hip joint angle are the system errors that can be eliminated by output gain (yellow circle). (b) The curve tracking of the knee joint is not accurate as of the hip joint, especially in the stance phase when the knee joint is extended (green circle), but the knee joint trajectory feature shows stable periodicity.

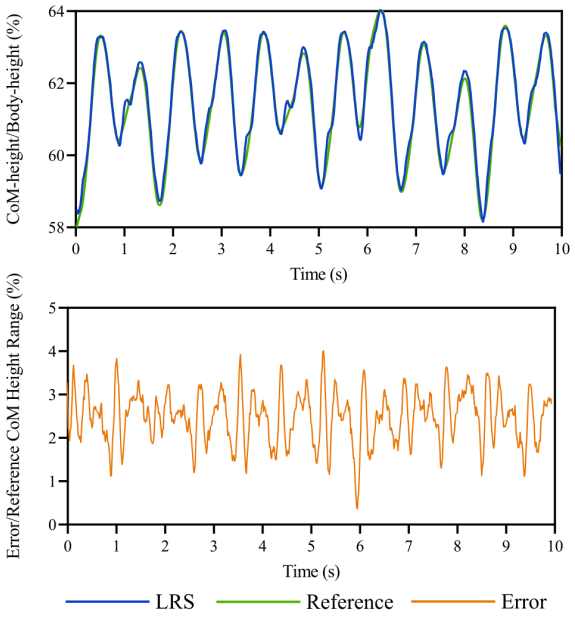

Fig. 6. The real-time CoM estimation by LSTM neural networks compared to reference values from the motion capture system with a healthy subject walking at 1 m/s.

the paretic Fig. 4 (a) and healthy (b) sides of the subject. The remaining five markers are not in either view of the two sub-figures. Besides, two markers are located on the same vertical level of venter and horizontal waist center for CoM height validation.

B. Experimental Data Processing

The data of five stable gait cycles are processed to verify the relationship between the calculation results of the locomotion recognition system and the reference values. The root mean square error (RMSE) $E(\theta)$ can be obtained by the following formula:

$$E(\theta) = \sqrt{\frac{1}{n} \times \sum_{i=1}^{n} (\theta_{LRS} - \theta_r)^2} \tag{13}$$

where θ_{LRS} are the joint angles calculated by the locomotion recognition system and θ_r are the reference angles collected by the motion capture system.

A one-way analysis of variance (ANOVA) was conducted to compare the effect of the different BWS strategies on gait phase, kinematic performance, and foot pressure, with significance set at $p \leq 0.05$.

IV. Results

A. Lower Limb Joint Angles Estimation

Three healthy subjects' walking data are used for evaluating the lower limb joint angles estimation. Fig. 5 indicates the comparison of the lower limb joint angles in five stable gait cycles calculated by the locomotion recognition system and motion capture system under the walking speed of 1m/s. Compared to the reference values, the RMSEs of the hip and knee joint angles obtained from the locomotion recognition system are 0.53° and 1.32°. The mean errors of peak and valley values in five gait cycles of the hip joint are 1.7°, which accounts for less than 4.82% of the hip joint angle range (as shown in yellow circles in Fig. 5(a)). In the rising and falling edge of joint angles trajectories, whose slopes are the joint velocities by backward difference calculation of angles trajectories, the curve tracking of the hip joint is more accurate than the knee joint by 20%, especially in the stance phase when the knee joint is extended (as shown in the green circle in Fig. 5(b)) for supporting the whole body weight. The RMSE of knee extension in the stance phase is 2.6°. However, considering the repeatability of joint error in this phase, it can be handled as an inherent system error in further application.

B. CoM Height Estimation

Fig. 6 shows the comparison between the CoM height normalized by the body height of a healthy subject (height 179 cm, leg-body height ratio 0.61) from the motion capture system and the one estimated from the proposed LSTM network during five continuous gait cycles at the walking speed of 1m/s. Notice that, the mean normalized displacement of the five gait cycles is 0.039. Compared to the reference values, the RMSE of the CoM height estimated by the trained LSTM is 3.19% (estimation err/reference CoM height range). The results demonstrate that the CoM height adjustment strategy with the LSTM network can effectively estimate the CoM height.

C. Gait Phase Improvement

The stance phases of the normal person's two sides have approximately the same duration in the over-ground walking,

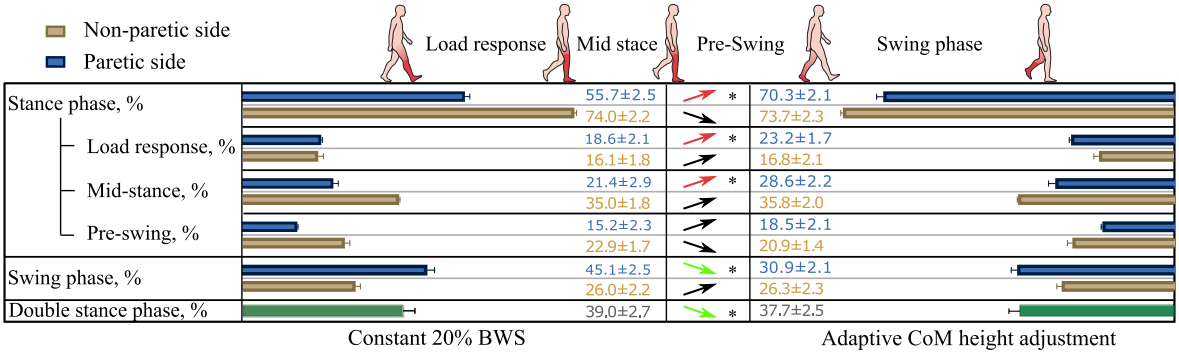

Fig. 7. Gait phase comparison between the constant partial BWS and variable CoM height adjustment strategy. H: paretic side, U: non-paretic side. The number of the phases refers to gait percentage. The adaptive CoM height adjustment significantly improved the standing phase of the paretic side of the patients and also improved the symmetry of the gait on both sides. The subphases of stance are extended at different levels. Especially, the load-response and mid-stance are significantly improved by more than 5.3% of the gait percentage. *significant, and $p < 0.05$.

while the stance phase of the paretic side is generally shorter than that of the healthy side due to the poor supporting ability of the injured side. Fig. 7 shows the gait phase comparison between the constant 20% partial BWS and CoM height adjustment strategy. Comparing the two body weight support strategies, the adaptive CoM height adjustment significantly increased the standing phase of the paretic side of the patients by 14.6% of the gait cycle ($p < 0.01$) and thus improved the symmetry of the gait on both sides. Further analysis of the data reveals that among the three subphases of stance, the middle stance is the most significant ($p < 0.05$), increasing by 25% one that undergoes the most significant ($p < 0.05$) increase (25%), suggesting that CoM height adjustment is effective in providing stabilizing assistance to patients during standing on the injured side. While the standing stage is prolonged, the swing stage is shortened. The mean difference between the two swing stages under constant BWS is 4.5% larger than that of CoM height adjustment in the whole gait cycle. This gait asymmetry is clearly observable during the walking training.

Data analysis found that the two body weight support strategies also have no significantly different effect on the non-paretic side. Except for the pre-swing phase, the proportion of other gait phases increased by 0.63% of the gait cycle, which is not significant ($p = 0.08$) for observation in walking.

D. Kinematic Parameters With Adaptive CoM Height Adjustment

To evaluate the different effects of the constant BWS and the CoM height adjustment strategies on kinematic performance, the paretic side's hip, knee joint angles of the hemiplegic subjects and healthy control group were recorded for comparison. Fig. 8 shows the comparison of the hip and knee joints angles (mean±SD) of hemiplegic subjects in two groups and healthy subjects under the two BWS strategies, respectively (twenty continuous gait cycles at 1m/s). The CoM height adjustment increases the mean hip and knee joints' range of motion of four subjects in the muscle strength Level IV group by 38.23% and 27.48%, respectively. The range of motion improvement of hip (29.61%) and knee (23.19%) joints can also be found in the Level III group. In general, the significant ascents ($p < 0.01$) of seven subjects' range of motion of hip and knee were 34.54% and 25.64%, respectively. Apart from the joint angle of lower limbs, the knee joint velocity is improved by 20°/s per gait cycle phase in the middle stance and pre-swing phase. The extension velocity improvement demonstrates that the knee joint is more flexible with less impedance under the CoM height adjustment training. For the healthy subjects, there is no significant difference ($p = 0.1$) in joint angles under the two BWS strategies, althought the hip and knee angles' mean range of motion are increased under VCHA by 10.31% and 6.58% compared with constant BWS, respectively. In the hip versus knee angle profiles, the heel strike transition of hemiplegic subjects (Level III and IV) is more stable with sufficient knee flexion under the VCHA strategy. For the healthy subjects, the two training strategies have no significantly different effect on the lower limb joints range of motion. Although there is knee flexion in the heel strike, the knee joint showed a relative delay under constant partial BWS, while the hip and knee motion under VCHA was more in line with a normal gait as shown in the hip versus knee angle profiles.

CoM height is an essential evaluation indicator for BWS treadmill training. The direct CoM height analysis lacks comparability because body height determines the mean CoM height. We took the CoM height to body height ratio as a parameter in data processing for analysis. The CoM height trajectory in a gait cycle is usually a peak-peak curve as shown in Fig. 6. The constant BWS training strategy fails to support the subjects to obtain a symmetrical CoM height as non-disabled subjects. The difference between the two peaks height to body height ratio of two groups under the constant BWS training is 0.043 and 0.021, while the CoM height to body height ratio adjustment can decrease the difference to 0.005 (third row of Fig. 8). The significant differences of the CoM to body height ratio with constant BWS and with CoM height adjustment were calculated through a one-way ANOVA ($p < 0.05$). The CoM height regulation by adaptive adjustment strategy is closer to the mean values of the 14 non-disabled

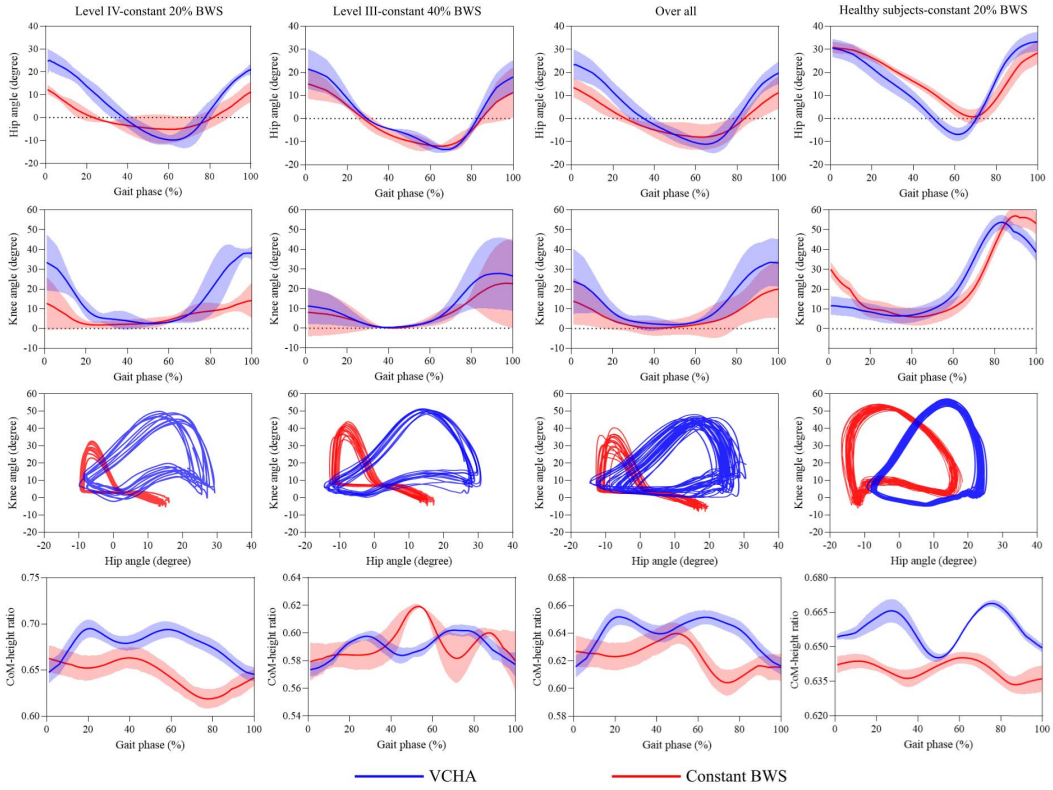

Fig. 8. Comparison of kinematic performance in the paretic side of subjects in Level IV, Level III and healthy subjects group during variable CoM height adjustment (VCHA) and constant BWS treadmill training. From top to bottom, it shows hip, knee joint angle, and CoM to body height ratio. The regulation strategy improves the hip and knee joints' range of motion and the knee joint veolocity in the middle stance and pre-swing phase for three subjects.

subjects. However, for the healthy subject, the mean CoM height under VCHA is significantly higher than constant BWS by 0.01 CoM to body height ($p < 0.01$). Besides, there a peak CoM height is 15% of gait phase hysteresis under constant BWS compared to VCHA.

E. Average Foot Pressure

Fig. 9 shows both sides's foot pressure (mean+SD) of the hemiplegic subject (S12) and a healthy subject (height: 167cm, weight: 61kg) collected by the pressure measuring insoles at constant BWS and the CoM height adjustment strategies. For the hemiplegic subject, the maximum foot pressure in common practice can be found in the middle of the stance phase. Instead, the maximum foot pressure of the paretic side appears in the pre-swing phase under the two strategies. It is found that the CoM height adjustment increases the maximum foot pressure by 45.67% compared to the constant BWS strategy. The difference of stance phase length between the paretic side and non-paretic side under the CoM height adjustment decreases by 12.5% compared to the constant BWS strategy ($p < 0.05$). Meanwhile, there is a significant difference between the stance and swing phase of the healthy side ($p < 0.05$). For the healthy subject, the gait phase symmetry is promoted by 3.1% of a gait cycle under the VCHA compared to the constant partial BWS while there is no significant variation in mean foot pressure ($p > 0.1$).

V. Discussion

The locomotion recognition system is the foundation of the CoM height estimation strategy. The theoretical proof of the convergence of the trained network for each subject was not investigated. Through experiments for healthy young people and hemiplegic subjects, the convergence was guaranteed, the convergence error of the trained neural network was bounded in a small range. For the training, the maximum fitting error was $2.43mm$ for eleven healthy young people. For the testing, the maximum fitting error was $3.37mm$ for three healthy people. We also considered the experiment for seven hemiplegic subjects, the maximum fitting error was 3.95mm. Despite some error between the calculated data by the locomotion recognition system and the reference data, the joint angle recognition results in Fig. 5(a, b) fully meet our training model's requirements and provides an accurate height estimation of the CoM height. This research is mainly investigating the nonlinear relationship between the lower limb joint angles and CoM height in time sequences. The LSTM network pays more attention to the periodicity of the input signal, which does not need to qualify with a highly precise measurement.

Gait disorders represent disabling symptoms in hemiplegic disease [4]. The effectiveness of rehabilitation treatment with BWS treadmill training has been demonstrated in patients with stroke, and spinal cord injuries [5]. The most important finding of this research is that the CoM height adjustment strategy with

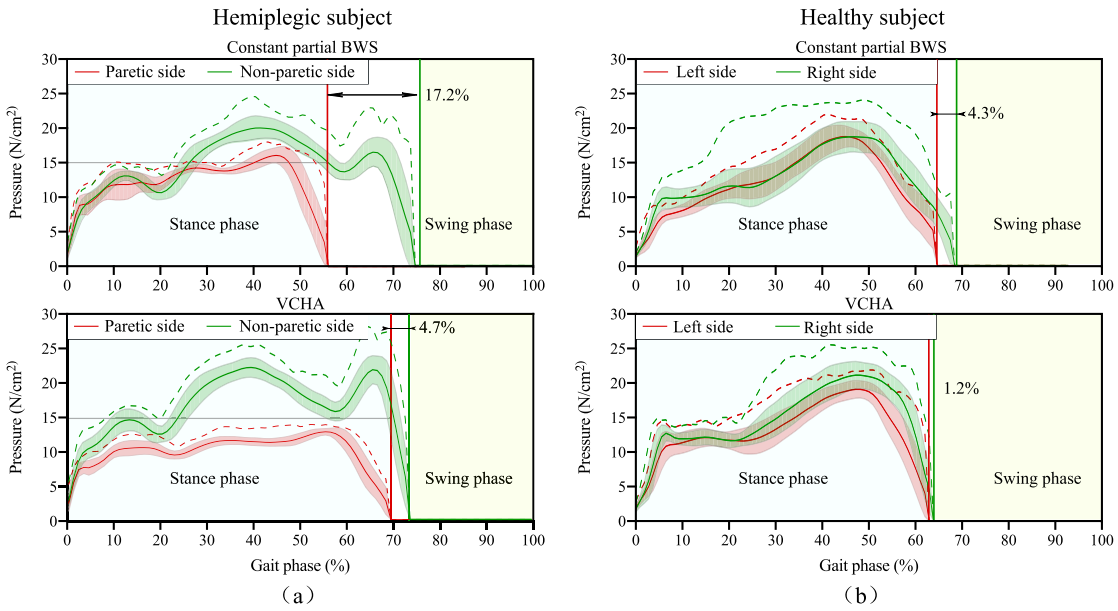

Fig. 9. (a) Hemiplegic subject: foot pressure (mean+SD) of hemiplegic and non-paretic side comparison between the constant partial BWS and VCHA treadmill walking training. The VCHA strategy gives an extended stance phase match for the paretic side and decreases the overall foot pressure. The less loading on the paretic side enables the lower joints to move with less resistance. (b) Healthy subject: foot pressure (mean+SD) of two side comparison between the constant partial BWS (20%) and VCHA treadmill walking training. The VCHA strategy does not affect the gait phase symmetry compared to the constant partial BWS.

motion capture of the non-paretic side significantly altered kinematics of the hip and knee joints during the stance phase, in addition to affecting the gait phase characteristics of the stride cycle and foot pressure. To our knowledge, this is the first attempt to adjust the CoM height on the basis of the active movement of the non-paretic side for the BWS treadmill training in post-stroke rehabilitation. The CoM height adjustment proposed in this study is a pure position control mode. With NaturaGait's powerful driving capability (rated lifting force of 1500N), subjects weighing between 50kg and 120kg can follow the target CoM height on the CoM height adjustment in the position loop. Constant partial BWS is an impedance force control, which adjusts the height of the man-machine connection by comparing the weight of the target weight loss support and the difference in the force sensor's actual value between the rehabilitation robot and the wearing harness. The BWSTT is mainly used to help subjects with weak muscle strength achieve stable walking training under the condition of reducing the load of the lower limbs. Continuous walking with approximately periodic CoM height guidance of BWS framework and the treadmill is an effective method for lower limbs in hemiplegic rehabilitation. Individuals with hemiplegia lack stability in walking, and this stability leads to discontinuity in the constant partial BWS training. The VCHA method actively adjusts the ideal CoM height which supports the subjects to walk sustainably. Thus, this method does not restrict the subject's BWS walking but is an orthopedic strategy for gait training.

It is clear from these results that significant changes occur, most notably an increase in hip and knee range of motion (Fig. 8), shorter swing phase, and more extended stance phase of paretic side), longer stride duration (Fig. 6. The CoM height adjustment strategy effectively improves the peak symmetry of the same gait period. This peak symmetry demonstrates the stability of the CoM during the subject's walking process. Also, it indicates that the height control of weight loss support can effectively improve the paretic side's active movement ability. Compared with constant 20% BWS, the dynamic adjustment of the CoM height in the standing period of the paretic side is more beneficial to the strength rehabilitation of the patient's knee joint. It is also the reason why CoM height adjustment can improve the range and speed of knee motion.

However, foot pressure results shown in Fig. 9 indicate that the maximum foot pressure under CoM height adjustment is less than constant BWS, which means that the paretic side does not obtain enough impedance for joint active rehabilitation training. This low impedance for the paretic side is a limitation of CoM height adjustment. The future work of CoM height adjustment will define the CoM height support ratio or combine CoM height adjustment with constant BWS to settle this matter.

Regarding the comfort level of BWS training, the constant weight support is easy to interfere with the gait of the subjects' paretic side [16]. However, there is load-free assistance when dragged by the wearable harness. The gait affects the metabolism and is responsible for fatigue increase during treadmill training. The effects of gait on energy expenditure and how to compare and evaluate different BWS strategies' performance in this regard needs to be studied.

VI. Conclusion

This paper investigates a strategy for variable CoM height adjustment to enhance the efficiency of BWS treadmill training of hemiplegic patients after stroke. The strategy we propose composes of a long-short term memory (LSTM) network and a locomotion recognition system. The LSTM network takes

the hip and knee joint angles of the hemiplegic patients' non-paretic side from the locomotion recognition system as input signals and outputs the CoM height to a BWS treadmill training robot. The locomotion recognition system has been proved to be accurate, with small RMSEs of the hip (0.53°) and knee (1.32°). With the adaptive CoM height adjustment strategy, the standing phase of the paretic side is increased by 14.6% of the gait cycle. Besides, the hip and knee joints' ranges of motion are increased by 38.23% and 27.48%, respectively. The difference between the two peaks under the constant BWS training is decreased by 46.03%, which demonstrated that the CoM height adjustment improves the gait stability. Considering the walking performance is different according to different ages, a comparative experiment will be carried out on trained models using the young people and age-matched population data of subjects respectively in the future.

ACKNOWLEDGMENT

The authors would like to thank C.R. Zhang, L. Xiao, and P. Xu from Sunshine Rehabilitation Center, Shanghai, China, for their contributions in experiments.

REFERENCES

[1] D. A. Bjanes and C. T. Moritz, "A robust encoding scheme for delivering artificial sensory information via direct brain stimulation," *IEEE Trans. Neural Syst. Rehabil. Eng.*, vol. 27, no. 10, pp. 1994–2004, Oct. 2019.

[2] G. Pavei, F. Salis, A. Cereatti, and E. Bergamini, "Body center of mass trajectory and mechanical energy using inertial sensors: A feasible stride?" *Gait Posture*, vol. 80, pp. 199–205, Jul. 2020.

[3] E. De Keersmaecker *et al.*, "The effect of optic flow speed on active participation during robot-assisted treadmill walking in healthy adults," *IEEE Trans. Neural Syst. Rehabil. Eng.*, vol. 28, no. 1, pp. 221–227, Jan. 2020.

[4] E. Swinnen *et al.*, "Walking with robot assistance: The influence of body weight support on the trunk and pelvis kinematics," *Disab. Rehabil., Assistive Technol.*, vol. 10, no. 3, pp. 252–257, May 2015.

[5] P. Zhang, W. Zou, Y. Chen, and N. Yu, "Servo and force control with improved robustness and accuracy for an active body weight support system," in *Proc. IEEE Int. Conf. Adv. Intell. Mechtron.*, Jul. 2019, pp. 601–605.

[6] K. Chua *et al.*, "An exploratory clinical study on an automated, speed-sensing treadmill prototype with partial body weight support for hemiparetic gait rehabilitation in subacute and chronic stroke patients," *Frontiers Neurol.*, vol. 11, p. 747, Jul. 2020.

[7] M. H. Rad and S. Behzadipour, "Design and implementation of a new body weight support (BWS) system," in *Proc. Int. Conf. Robot. Mechatronics*, Oct. 2017, pp. 69–75.

[8] M. A. Ullah, H. Shafi, G. A. Khan, A. N. Malik, and I. Amjad, "The effects of gait training with body weight support (BWS) with no body weight support (no-BWS) in stroke patients," *J. Pak. Med. Assoc.*, vol. 67, no. 7, pp. 1094–1096, 2017.

[9] R. S. Gonçalves and H. I. Krebs, "MIT-Skywalker: Considerations on the design of a body weight support system," *J. NeuroEng. Rehabil.*, vol. 14, no. 1, pp. 1–11, Dec. 2017.

[10] A. C. Dragunas and K. E. Gordon, "Body weight support impacts lateral stability during treadmill walking," *J. Biomech.*, vol. 49, no. 13, pp. 2662–2668, Sep. 2016.

[11] K. Dyer, B. King, and A. Herman, "A new body weight supported treadmill device to measure kinetic response from spinal cord injury animals," in *Proc. IEEE Annu. Northeast Bioeng. Conf.*, Apr. 2015, pp. 1–2.

[12] K.-M. Lee and D. Wang, "Design analysis of a passive weight-support lower-extremity-exoskeleton with compliant knee-joint," in *Proc. IEEE Int. Conf. Robot. Automat.*, May 2015, pp. 5572–5577.

[13] H. Munawar and V. Patoglu, "Gravity-assist: A series elastic body weight support system with inertia compensation," in *Proc. IEEE/RSJ Int. Conf. Intell. Robots Syst.*, Oct. 2016, pp. 3036–3041.

[14] J. A. Mercer and C. Chona, "Stride length–velocity relationship during running with body weight support," *J. Sport Health Sci.*, vol. 4, no. 4, pp. 391–395, Dec. 2015.

[15] H. Zhang, F. Mo, L. Wang, M. Behr, and P. J. Arnoux, "A framework of a lower limb musculoskeletal model with implemented natural proprioceptive feedback and its progressive evaluation," *IEEE Trans. Neural Syst. Rehabil. Eng.*, vol. 28, no. 8, pp. 1866–1875, Aug. 2020.

[16] M. Neal, N. Fleming, L. Eberman, K. Games, and J. Vaughan, "Effect of body-weight-support running on lower-limb biomechanics," *J. Orthopaedic Sports Phys. Therapy*, vol. 46, no. 9, pp. 784–793, Sep. 2016.

[17] M. Bannwart, S. L. Bayer, N. König Ignasiak, M. Bolliger, G. Rauter, and C. A. Easthope, "Mediolateral damping of an overhead body weight support system assists stability during treadmill walking," *J. NeuroEng. Rehabil.*, vol. 17, no. 1, pp. 1–15, Dec. 2020.

[18] D. J. Lura, M. C. Venglar, A. J. van Duijn, and K. R. Csavina, "Body weight supported treadmill vs. overground gait training for acute stroke gait rehabilitation," *Int. J. Rehabil. Res.*, vol. 42, no. 3, pp. 270–274, 2019.

[19] Y.-R. Mao *et al.*, "The effect of body weight support treadmill training on gait recovery, proximal lower limb motor pattern, and balance in patients with subacute stroke," *BioMed Res. Int.*, vol. 2015, pp. 1–10, 2015.

[20] J. Taborri, S. Rossi, E. Palermo, F. Patane, and P. Cappa, "A novel HMM distributed classifier for the detection of gait phases by means of a wearable inertial sensor network," *Sensors*, vol. 14, no. 9, pp. 16212–16234, 2014.

[21] N. Cespedes, M. Munera, C. Gomez, and C. A. Cifuentes, "Social human-robot interaction for gait rehabilitation," *IEEE Trans. Neural Syst. Rehabil. Eng.*, vol. 28, no. 6, pp. 1299–1307, Jun. 2020.

[22] M. Iosa, G. Morone, and M. Bragoni, "Driving electromechanically assisted gait trainer for people with stroke," *J. Rehabil. Res. Develop.*, vol. 48, no. 2, pp. 135–145, 2011.

[23] A. Schicketmueller, G. Rose, and M. Hofmann, "Feasibility of a sensor-based gait event detection algorithm for triggering functional electrical stimulation during robot-assisted gait training," *Sensors*, vol. 19, no. 21, p. 4804, Nov. 2019.

[24] A. Naidu, S. A. Graham, and D. A. Brown, "Fore-aft resistance applied at the center of mass using a novel robotic interface proportionately increases propulsive force generation in healthy nonimpaired individuals walking at a constant speed," *J. NeuroEng. Rehabil.*, vol. 16, no. 1, pp. 1–11, Dec. 2019.

[25] K.-R. Mun, Z. Guo, and H. Yu, "Restriction of pelvic lateral and rotational motions alters lower limb kinematics and muscle activation pattern during over-ground walking," *Med. Biol. Eng. Comput.*, vol. 54, no. 11, pp. 1621–1629, Nov. 2016.

[26] L. Tesio and V. Rota, "The motion of body center of mass during walking: A review oriented to clinical applications," *Frontiers Neurol.*, vol. 10, p. 999, Sep. 2019.

[27] F. Fallahtafti, C. M. Pfeifer, T. W. Buster, and J. M. Burnfield, "Effect of motor-assisted elliptical training speed and body weight support on center of pressure movement variability," *Gait Posture*, vol. 81, pp. 138–143, Sep. 2020.

[28] P. Esser, H. Dawes, J. Collett, and K. Howells, "IMU: Inertial sensing of vertical CoM movement," *J. Biomechanics*, vol. 42, no. 10, pp. 1578–1581, Jul. 2009.

[29] D. Steins, I. Sheret, H. Dawes, P. Esser, and J. Collett, "A smart device inertial-sensing method for gait analysis," *J. Biomechanics*, vol. 47, no. 15, pp. 3780–3785, Nov. 2014.

[30] T. Zhen, L. Yan, and P. Yuan, "Walking gait phase detection based on acceleration signals using LSTM-DNN algorithm," *Algorithms*, vol. 12, no. 12, p. 253, Nov. 2019.

[31] T. N. Sainath, O. Vinyals, A. Senior, and H. Sak, "Convolutional, long short-term memory, fully connected deep neural networks," in *Proc. IEEE Int. Conf. Acoust., Speech Signal Process. (ICASSP)*, Apr. 2015, pp. 4580–4584.

[32] B. Su and E. M. Gutierrez-Farewik, "Gait trajectory and gait phase prediction based on an LSTM network," *Sensors*, vol. 20, no. 24, p. 7127, Dec. 2020.